NeuroImage 283 (2023) 120425

Contents lists available at ScienceDirect

NeuroImage

journal homepage: www.elsevier.com/locate/ynimg

The roles of edge-based and surface-based information in the dynamic neural representation of objects

Liansheng Yao [a,b], Qiufang Fu [a,b,*], Chang Hong Liu [c]

[a] State Key Laboratory of Brain and Cognitive Science, Institute of Psychology, Chinese Academy of Sciences, Beijing, China
[b] Department of Psychology, University of Chinese Academy of Sciences, Beijing, China
[c] Department of Psychology, Bournemouth University, Fern Barrow, Poole, UK

ARTICLE INFO

Keywords:
Neural representation of objects
Edge-based information
Surface-based information
EEG
MVPA

ABSTRACT

We combined multivariate pattern analysis (MVPA) and electroencephalogram (EEG) to investigate the role of edge, color, and other surface information in the neural representation of visual objects. Participants completed a one-back task in which they were presented with color photographs, grayscale images, and line drawings of animals, tools, and fruits. Our results provide the first neural evidence that line drawings elicit similar neural activities as color photographs and grayscale images during the 175–305 ms window after the stimulus onset. Furthermore, we found that other surface information, rather than color information, facilitates decoding accuracy in the early stages of object representations and affects the speed of this. These results provide new insights into the role of edge-based and surface-based information in the dynamic process of neural representations of visual objects.

1. Introduction

It is well known that people can easily recognize objects in line drawings, even though they contain only edge-based information. In the real world, however, objects are defined not only by their edges, but also by surface information such as color, texture, and luminance gradient. So how does the human brain readily recognize objects in such different forms as being the same objects? What are the roles of edge-based and surface-based information in neural representation of objects?

There are two competing theories about object coding. The edge-based theory proposes that edge information alone is sufficient for object recognition and discrimination, while surface information serves as a secondary source for recognition (Biederman and Ju, 1988). Indeed, some studies have demonstrated that color and textures of objects do not improve recognition accuracy when images are presented briefly (Cave et al., 1996; Fu et al., 2016). Moreover, line drawings and color photographs of natural scenes seem to elicit similar patterns of activation in the brain areas, such as the parahippocampal place area (PPA) and the retrosplenial cortex (RSC) (Walther et al., 2011). These findings provide evidence for the edge-based theory and suggest that edge-based information plays a primary role in neural representation of objects.

However, others have argued that both edge-based and surface-based information are equally important (Parron and Washburn, 2010). For example, when objects or scenes have no color or inconsistent color, recognition accuracy could be compromised (Gegenfurtner and Rieger, 2000; Goffaux et al., 2005; Schyns and Oliva, 1994; Wurm et al., 1993). Changing the texture of scene images can also impair the judgments of scene layout (Robin et al., 2017). Moreover, an fMRI study revealed that both edge-based and surface-based information are equally weighted in the PPA, indicating that both types of information play equally an important role in scene recognition (Lowe et al., 2017). These findings contradict the edge-based theory but provide supporting evidence for the surface-based theory.

Moreover, it remains controversial whether the edge information receives higher priority in object recognition. Some studies have supported the idea that edge-based information receives higher priority in object recognition and surface-based information does not affect or slow down the speed of recognition (Fu et al., 2016; Martinovic et al., 2008). On the other hand, others have found that when the objects devoid of color or with inconsistent color can slow down the speed of recognition performance (Goffaux et al., 2005).

There may be three reasons for these seemingly contradictory findings. Firstly, the type of objects can determine the level of contribution from surface-based and edge-based information (Laws, 2001). For

* Corresponding author at: Institute of Psychology, Chinese Academy of Sciences, 16 Lincui Road, Chaoyang District, Beijing 100101, China.
E-mail address: fuqf@psych.ac.cn (Q. Fu).

https://doi.org/10.1016/j.neuroimage.2023.120425
Received 19 May 2023; Received in revised form 22 October 2023; Accepted 24 October 2023
Available online 27 October 2023

example, color and surface information play a more prominent role in recognizing fruits than recognizing animals or tools, whereas edge-based information is more important for recognizing animals than for recognizing fruits (Cree and McRae, 2003; Rossion and Pourtois, 2004). Secondly, the stimulus exposure time can modulate the role of edge-based and surface-based information. A longer exposure time results in higher recognition accuracy for color photographs than for line drawings (Fu et al., 2016; Laws and Hunter, 2006). Finally, the level of abstraction can also influence the role of the two types of information. For example, edge information is sufficient for the processing at a superordinate level (e.g., identifying a bird as an 'animal'), while surface information is needed for the processing at a basic level (e.g., 'bird') or subordinate level (e.g., 'eagle') (Price and Humphreys, 1989; Zachariou et al., 2018). Thus, these three factors need to be factored while investigating the roles of edge-based and surface-based information evolve over time.

Crucially, neural representation of objects is a dynamic process. However, it remains unclear how the two information types play different roles during the time courses of object processing. Previous studies mainly conducted univariate analysis of EEG data and focused on specific event related potentials (ERPs). For example, the information about shape and color can regulate the P1 and N1 amplitudes at 80 and 170 ms after stimulus onset over the occipital lobe (Redmann et al., 2014; Scholl et al., 2014). The combination of shape and color information can affect the P2 amplitude at 225 ms over the occipital lobe (Lloyd-Jones et al., 2012), and the complexity of stimulus pictures can influence the P3 amplitude at 250-500 ms over the parieto-occipital lobe (Hu et al., 2022). However, it has been argued that the focuses on a few prominent ERP components may provide an incomplete or possibly misleading view of the dynamic processing of objects in the brain (Rousselet and Pernet, 2011). Therefore, it remains unclear how the neural activity elicited by edge- or surface-based information evolves over time in object neural representations.

Recently, to investigate the dynamic development of neural representations in the brain, more and more studies have used the MVPA on time-sensitive neuroimaging data such as EEG or MEG (Cichy et al., 2014; Grootswagers et al., 2017; Proklova et al., 2019; Sanchez et al., 2020; Smith and Smith, 2019). The MVPA possesses a higher sensitivity compared to traditional univariate analysis in that MVPA can analyze the whole brain activation patterns corresponding to different conditions and detect the differences in activation. These differences might be lost in univariate analysis methods which rely on averaged signals (de-Wit et al., 2016; Hatamimajoumerd et al., 2022). Importantly, the MVPA enables exploration of object representations across the entire brain, providing a more comprehensive understanding of neural processing (Contini et al., 2017). It has been found that visual objects can be decoded from full channel MEG about 80-100 ms after the stimulus onset (Carlson et al., 2013; Cichy et al., 2014), color features can be decoded from about 70 ms after the stimulus onset (Teichmann et al., 2020). The MVPA analysis can thus provide important insights into the role of edge-based and surface-based information in the dynamic development of the neural representation of visual objects.

Therefore, the present study combined MVPA with EEG to explore how neural representations for edge-based and surface-based information evolve over time. We adopted images of animals, fruits, and tools as stimuli because of prior finding that edge-based and surface-based information may play different roles in recognizing these categories. Also, because surface-based information plays a greater role at the subordinate level of categorization with brief stimulus exposure (Fu et al., 2016; Laws and Hunter, 2006), we presented subordinate-level stimuli for 200 ms in each trial of this study. Participants completed a one-back task, in which they were asked to press a button when an image repeated a previous trial. To distinguish the role of contour, color, and other surface information, each object was shown in three versions: color photographs, grayscale images, and line drawings (Boshyan et al., 2018; Teichmann et al., 2020). Line drawings contained only edge-based information, while grayscale images and color photographs consisted of both edge- and surface-based information but varied only in color.

We used time-resolved decoding to explore the neural representations for different versions of stimuli. If all three versions of stimuli elicited comparable neural activities at different time courses, it would suggest that a similar neural representation was involved in decoding these stimuli, and the edge-based information was likely to be sufficient. Alternatively, if the stimuli created different neural activities at certain time points, it would indicate that color or other surface information influenced object representations at those points. Further, we also used the time generalization analysis to verify whether neural activities for grayscale images were similar to those for color photographs and line drawing over a range of time courses. If generalization accuracy were better than the chance level, it would indicate that the structure of the multidimensional space for different types of images was comparable at these time courses. Moreover, if the significant points shifted away from the diagonal, it would indicate that the time of information processing for the two types of images was asynchronous, and vice versa.

2. Methods

2.1. Participants

Twenty participants (10 female, mean age 23.5 years, SD = 2.0) with normal or corrected-to normal vision participated in the study. The sample size was determined according to similar studies conducted in the past (Cichy et al., 2014; Proklova et al., 2019; Smith and Smith, 2019; Teichmann et al., 2020). All were paid for their participation and provided informed consent before the experiment. The experiment was approved by the Institutional Review Board of the Institute of Psychology, Chinese Academy of Sciences.

2.2. Stimuli and Apparatus

The stimuli consisted of three categories of animals, fruits, and tools, with 12 objects in each category. Each object had three versions: color photographs, grayscale images, and line drawings, resulting in a total of 108 images (see Fig. 1A). All images had a resolution of 480 × 480 pixels. Grayscale images were generated from color photographs using MATLAB R2021b (www.mathworks.com), while line drawings were produced by trained artists who traced neutral the contours in color photographs with neutral gray lines using a customized graphical user interface. Stimulus presentation was controlled using Psychtoolbox 3 for MATLAB (Brainard, 1997; Kleiner, 2010).

2.3. Procedure

The participant's viewing distance was 60 cm from the screen. Each stimulus image subtended 5 × 5 degrees of visual angle. A fixation cross was presented on a neutral gray background in the center of the screen throughout the trials. On each trial, an object image was presented for 200 ms followed by a variable interstimulus interval of 900-1100 ms (see an example in Fig. 1B). Participants performed a one-back task, in which they were instructed to view the images and press a button when an image was repeated. The next trial began, regardless of whether there was a response. To avoid artifacts caused by eye movements, participants were required to fixate on a central fixation cross in the center of the screen throughout the experiment.

The experiment consisted of 30 blocks, with a total of 4,050 trials. Each block contained 135 trials, in which the 108 object images were presented in a random order, and 27 of them were randomly selected to appear twice in two consecutive trials. The 27 target trials were used to maintain the participant's attention and were not included in the EEG data analysis.

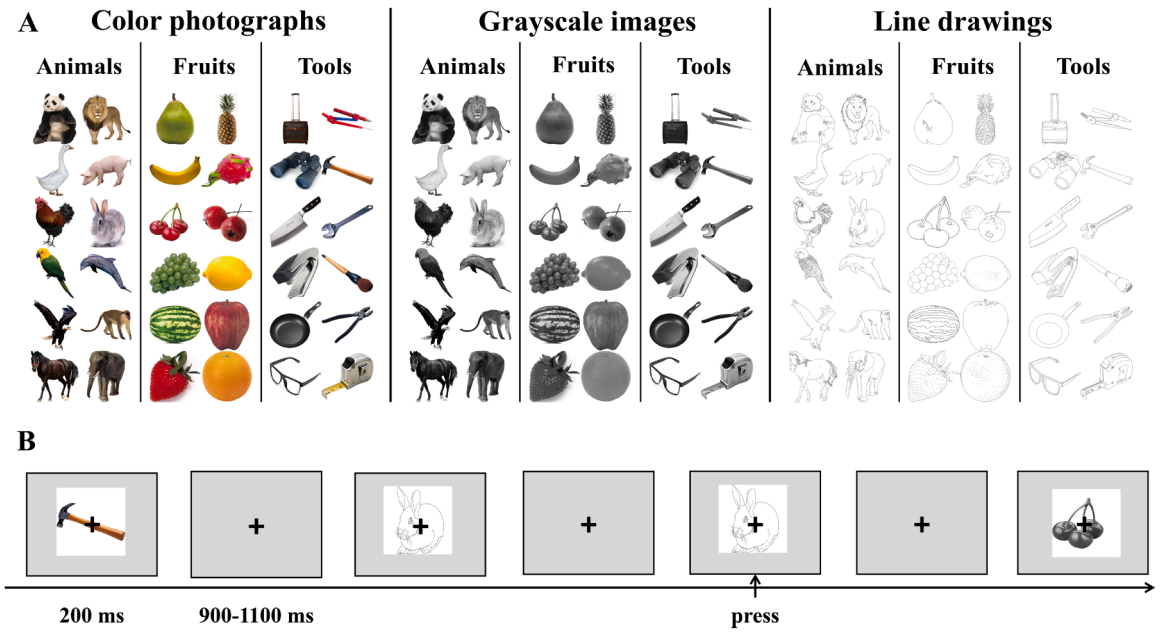

Fig. 1. Stimuli and experimental procedure. (A) All stimuli were used in this experiment. There were three categories of objects: animals, fruits, and tools. Each object had three versions: color photographs, grayscale images, and line drawings. (B) An example sequence of the trial procedure. Participants viewed object images and were asked to press a button when an image was repeated on two consecutive trails (such as the rabbit in this example).

2.4. EEG acquisition and preprocessing

EEG data were collected using a 64-channel neuroscan system with a 1000 Hz sampling rate. The left mastoid was used as an online reference, and the right mastoid was used as an offline re-reference. Data were pre-processed offline using MATLAB and EEGLAB Toolbox (Delorme and Makeig, 2004). We extracted trials from -100 to 800 ms relative to stimulus onset. Each trial was baseline-corrected by subtracting mean amplitude during the period 100 ms prior to stimulus onset. Data were filtered using a 0.1-30 Hz pass. The ICA was used to detect and remove blink shadows and other motion related shadows. The trials of excessive artifacts (peak-to-peak deflection exceeding ±100 μV) and wrong response were rejected, accounted for 7.9 % of all the trials. The EEG data were down-sampled to 200 Hz to reduce the processing time and improve the signal-to-noise ratio (Grootswagers et al., 2017).

2.5. Behavioral performance

The false alarms, sensitivity index (*d'*), and bias (*c*) scores were calculated according to the signal detection theory (Macmillan and Creelman, 1991). The response time (RT) was defined as the duration from the stimulus onset to a key press in hit responses. We conducted a two-way repeated-measures analysis of variance (ANOVA) with 3 (object types: animals, fruits, and tools) × 3 (image versions: color photographs vs. grayscale images vs. line drawings) for these measures. The Greenhouse-Geisser correction was used to correct the *P*-value, and the Bonferroni correction was used for post-hoc comparisons. Simple effect analysis was conducted on interaction effects.

2.6. EEG analysis

Time-resolved decoding. To examine the role of edge-based and surface-based information in neural representation of objects, the time-resolved decoding was conducted through the linear support vector machine (SVM, libsvm) classifier (Chang and Lin, 2011) as it is commonly used in previous studies (Cichy et al., 2014; Dobs et al., 2019; Smith and Smith, 2019) on the EEG data of color photographs, grayscale images, and line drawings. The classifier utilized the default parameters from the CoSMoMVPA toolbox (Oosterhof et al., 2016). For each version of image, there were 36 pictures, and each of them was paired with every other picture in the set. This resulted in a total of 630 pairs (36 × 35/2 pairs). The cross-validated pairwise classification accuracy of the SVM was used to obtain the similarity measure of each pair. A time window of 10 ms and a step size of 5 ms were used when conducting the classification analysis (Grootswagers et al., 2017). The analysis was performed separately for each participant in a time-resolved manner (see Fig. 2). Firstly, we divided all the trials of each picture into ten groups. Nine groups were selected randomly as the training set and one group as the testing set (i.e., ten-fold cross-validation). Then, all 630 pairs were binary classified, and the classification process was repeated 100 times. The average decoding accuracy of 100 times was taken as the value of the 36 × 36 decoding matrix, which was called the representation dissimilarity matrix (RDM). This matrix was symmetrical, and the diagonal was not defined. Each participant and each time point needed an RDM. Like other prior research that employed this method (Cichy et al., 2014; Proklova et al., 2019; Teichmann et al., 2020), our aim was not to achieve the highest possible decoding accuracy but to evaluate whether the classifier can decode information from neural signals better than chance.

Spatial decoding classification analysis. To assess which electrodes contributed to the classification performance of color photographs, grayscale images, and line drawings within which time windows, an additional spatial classification analysis was conducted. In the analysis, binary decoding analysis was carried out for each electrode independently. With a time window of 60 ms and a step of 60 ms, we created a topographic map to display the decoded object information under a specific time window (Nemrodov et al., 2016; Smith and Smith, 2019).

Time generalization analysis. This was used to further investigate whether there was a similar activity pattern for the three types of images. At each time point of the activated EEG signal, a classifier was trained using the grayscale images and tested with the EEG for the same objects of color photographs and line drawings at all time points separately. This resulted in two 900 × 900 matrices (-100–800 ms to stimulus onset) that captured the classifier generalization performance across time. If the classifier trained at one time point could predict the class labels of test data at other time points, it would indicate a similar

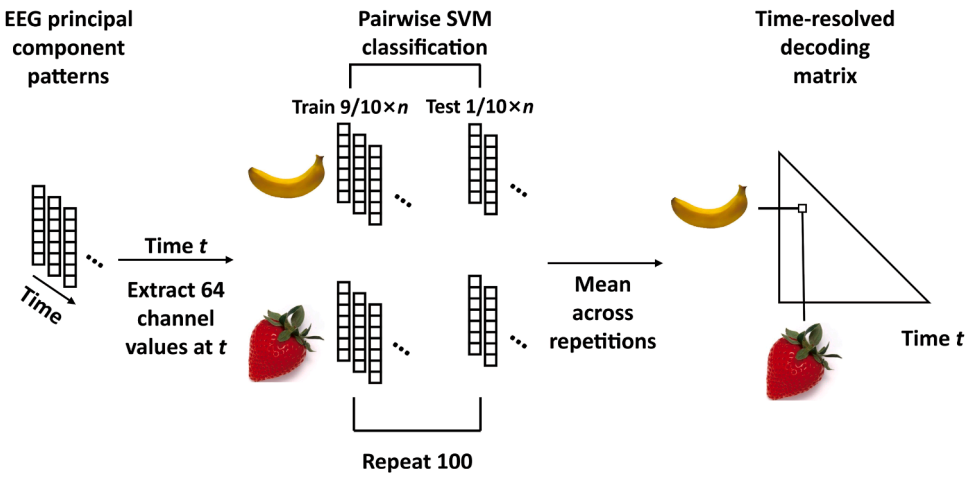

Fig. 2. For each participant, the time-resolved decoding was performed on the principal components (PCs) extracted from all EEG electrodes. For each time point *t*, the response pattern across PCs was extracted for each trial in each condition, followed by pairwise cross-validated SVM classification. The resulting decoding accuracy values resulted in a 36 × 36 representational dissimilarity matrix (RDM) for each time point.

structure of multidimensional space between training and testing. Otherwise, it would suggest a qualitative difference in the multidimensional space. The diagonal of the matrices corresponded to the standard time-resolved decoding results. The decodable non-diagonal effect reflected the temporal asynchrony of information processing in the training set and the testing set.

Statistical analysis. For the EEG data analysis, we employed threshold-free cluster enhancement (TFCE) (Smith and Nichols, 2009) to identify the periods when decoding accuracy was significantly above chance. This method used a cluster-based approach for multiple comparison correction and was implemented in the CoSMoMVPA toolbox. First, we conducted permutation tests, shuffling the trial labels, and for each participant, we re-ran the decoding analysis with these shuffled labels 100 times, thereby creating a null distribution for each participant. Then, we used Monte Carlo sampling to create a group-level null distribution by performing 1000 permutations with shuffled labels (Stelzer et al., 2013). The TFCE constructed an empirical distribution of the maximum cluster size in a threshold-free manner, with the threshold set at the 95th percentile of the distribution (i.e., equivalent to $p < 0.05$, one-tailed).

We employed bootstrap test to estimate the onset latency of object representations (i.e., the first significant time point post-stimulus), the peak latency (i.e., the time at which the maximum value) in the time-resolved decoding, and the training and testing times corresponding to the maximum decoding accuracy in the time-generalization decoding. To achieve this, we first bootstrapped the decoding accuracy of participants 10,000 times for both time-resolved analysis and time-generalization analysis. This yielded empirical distributions for onset latency and peak latency, from which the 95 % confidence intervals (CIs) were determined. To compare the variations in the onset and peak latencies among different image versions and the differences between training and testing times corresponding to the maximum decoding accuracy in the time-generalization decoding, we calculated the differences in latency across these 10,000 bootstrap samples between datasets, yielding an empirical distribution of latency differences. The p-value of a two-tailed test was defined by the number of differences lower or greater than 0 in the empirical distribution, divided by the number of permutations. Using false discovery rate (FDR) correction, a latency difference was considered significant if the 95 % CI did not encompass 0.

3. Results

3.1. Behavioral results

Results for false alarms, *d'*, *c*, and RTs are shown in Fig. 3. False alarms were of particular interest because we wanted to find out whether consecutive presentation of same object identity in a different image version was the main cause of the errors. ANOVA for these data showed significant main effects of object type, $F(2,38) = 9.546$, $p = 0.001$, $\eta_p^2 = 0.334$, and of image version, $F(2,38) = 7.378$, $p = 0.002$, $\eta_p^2 = 0.28$. These were qualified by a significant interaction (see Fig. 3A), $F(4,76) = 3.588$, $p = 0.014$, $\eta_p^2 = 0.159$. Further analysis revealed that the main cause of the false alarms was due to consecutive presentation of the same object with a different image version, accounting for 59 % of all false alarms. For example, presenting an object in color followed by the same object in grayscale or vice versa constituted 42 % of all false alarms, with tools accounting for 24 %, animals 15 %, and fruits for 3 %. This demonstrates that color is less diagnostic for tools and animals than for fruits. In addition, consecutive presentation of the same image version and object type accounted for 13 % of all false alarms, while same object type alone accounted for 9 %, and same image version alone accounted for 8 %. These results suggest that it was the recognition of the object's identity rather than low-level features, that affected the false alarm results. Specifically, the recognition of identical objects with different image versions contributed significantly to this behavioral measure.

For the *d'*, there were significant main effects of object type, $F(2, 38) = 7.408$, $p = 0.003$, $\eta_p^2 = 0.281$, and image version, $F(2, 38) = 3.516$, $p = 0.043$, $\eta_p^2 = 0.156$. Post-hoc comparison showed that animals scored higher than tools ($p < 0.001$), but no significant difference was observed between fruits and the other two object categories ($ps > 0.05$). Color photographs scored higher than grayscale images ($p = 0.034$), but no significant difference was found between line drawings and color photographs or between line drawings and grayscale images ($ps > 0.05$). The interaction between these did not reach significance, $F(4,76) = 1.89$, $p = 0.14$, $\eta_p^2 = 0.09$.

For the *c*, we also found significant main effects of object type, $F(2,38) = 14.237$, $p < 0.001$, $\eta_p^2 = 0.428$, and image version, $F(2,38) = 8.626$, $p = 0.001$, $\eta_p^2 = 0.312$. Post-hoc comparison showed a more liberal response bias for animals than for fruits ($p = 0.001$) or tools ($p = 0.001$), but results for fruits and tools were comparable ($p = 1$). Response bias for Color photographs was more liberal than grayscale images ($p = 0.001$) or line drawings ($p = 0.01$), but results for grayscale images and line drawings comparable ($p = 1$). Again, the interaction

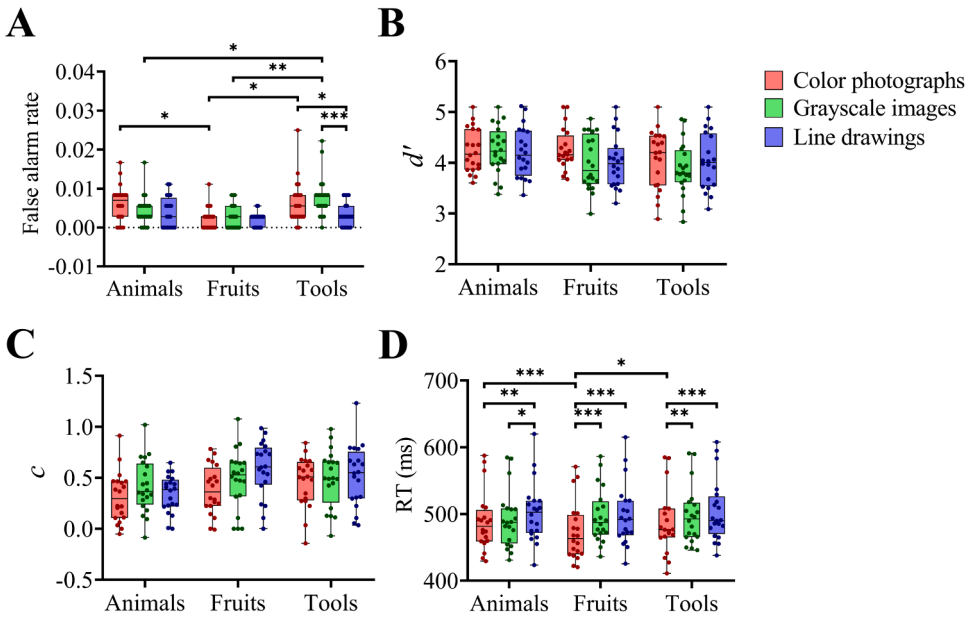

Fig. 3. Boxplots of behavioral results: (A) Results for False alarm rate, (B) Results for Sensitivity, (C) Results for Bias, and (D) Results for RT as a function of object type and image version. $^{*}p < 0.05$, $^{**}p < 0.01$, $^{***}p < 0.001$.

between these did not reach significance, $F(4,76) = 0.2604$, $p = 0.056$, $\eta_p^2 = 0.121$.

Similarly, an ANOVA on RTs revealed significant main effects of object type, $F(2,38) = 6.086$, $p = 0.006$, $\eta_p^2 = 0.243$, image version, $F(2,38) = 23.726$, $p < 0.001$, $\eta_p^2 = 0.555$, as well as a significant interaction, $F(4,76) = 4.217$, $p = 0.009$, $\eta_p^2 = 0.182$. Simple effect analysis by object type showed faster RTs for fruits than for animals ($p < 0.001$) and tools ($p = 0.012$) for color photographs only. Moreover, simple effect analysis by image version revealed faster RTs for color photographs than for line drawings for all three object types (all $ps < 0.05$).

3.2. Results of time-resolved decoding

To examine the role of edge-based and surface-based information in object representations, the time-resolved decoding method was used to analyze the EEG responses to color photographs, grayscale images, and line drawings. As shown in Fig. 4A, all types of object pictures were decoded accurately. The decoding accuracy grew significantly above

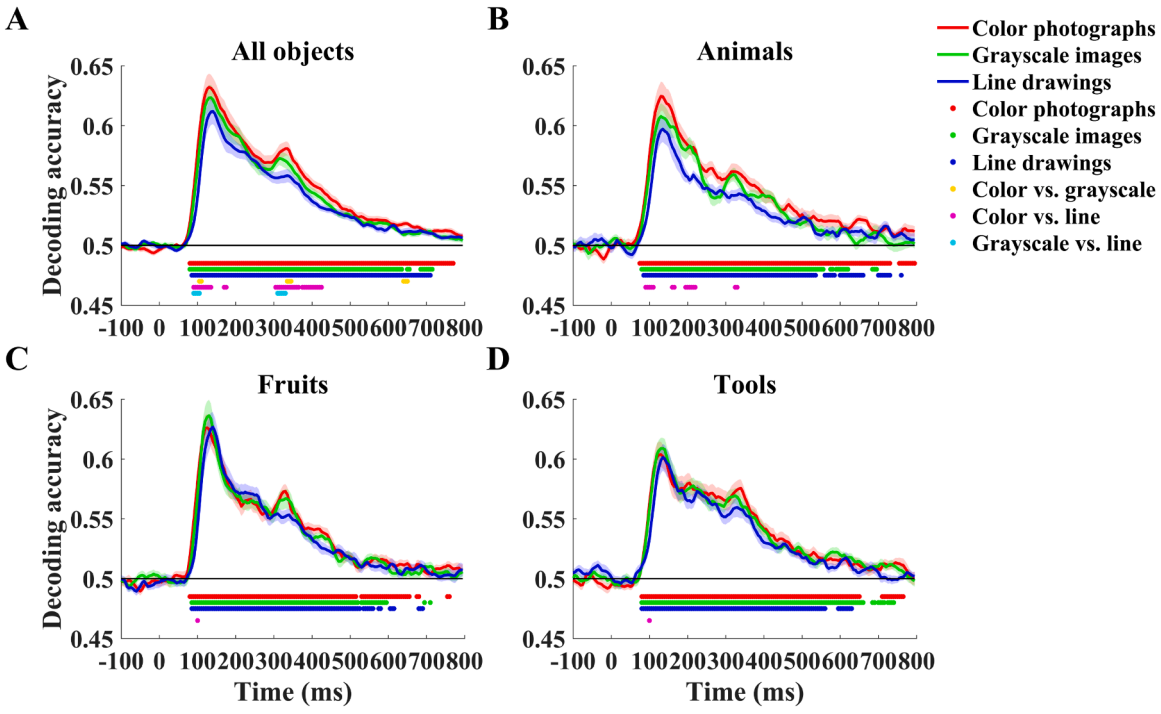

Fig. 4. The time courses of picture decoding for All objects (A), Animals (B), Fruits (C), and Tools (D). The red, green, and blue points below the plots indicate the time points when decoding accuracy was significantly better than chance (TFCE, corrected significance level $p < 0.05$). The yellow, magenta, and cyan line segments represent significant differences in decoding accuracy between color photographs and grayscale images, color photographs, and line drawings and grayscale images and line drawings, respectively. The shaded areas represent one SE about the means.

chance from 80-85 ms after the stimulus onset, peaked at 130-140 ms, and remained significant for a prolonged period. Specifically, the decoding accuracy reached significance at 80 ms for color photographs, 80 ms for grayscale images, and 85 ms for line drawings. The accuracy reached the peak at 135 ms for color photographs, 130 ms for grayscale images, and 140 ms for line drawings.

To test whether there was any difference in the time course of decoding of color photographs, grayscale images, and line drawings, the TFCE was used to compare the decoding accuracy between any two types of images (all *ps* < .05). Results revealed that the decoding accuracy for color photographs was significantly higher than grayscale images (yellow points in Fig. 4A) in the time windows of 105-110 ms, 335-345 ms and 640-650 ms. Decoding accuracy for color photographs was also higher than line drawings (magenta points) in the time windows of 90-135 ms, 170-175 ms and 305-425 ms. Decoding accuracy for grayscale images was significantly higher than line drawings during the 90-105 ms and 310-330 ms. No significant difference was found among the three versions of images during the time window of 175-305 ms, indicating that similar neural representations were elicited by the three versions of images during this period. Interestingly, a second peak at 315-335 ms was observed, where decoding accuracies for color photographs and grayscale images were again higher than the line drawings, indicating that surface information further improved decoding accuracy at this processing stage.

To assess the role of surface-based and edge-based information in different types of objects, we calculated decoding accuracy separately for each version of images for different types of objects (see Fig. 4B, C, and D). Results showed that in the early stage of object recognition (about 100 ms), decoding accuracy for animals, fruits, and tools was significantly higher in color photographs than in line drawings, but no significant difference was found between color photographs and grayscale images, or between line drawings and grayscale images. During the second peak, animals were decoded more accurately in color photographs than in line drawings.

The bootstrap test was used to estimate the onset and peak latency of time-course decoding for different types of images (Fig. 5A). There was no significant difference among the three image versions. We also estimated the onset latency and peak latency for different object categories

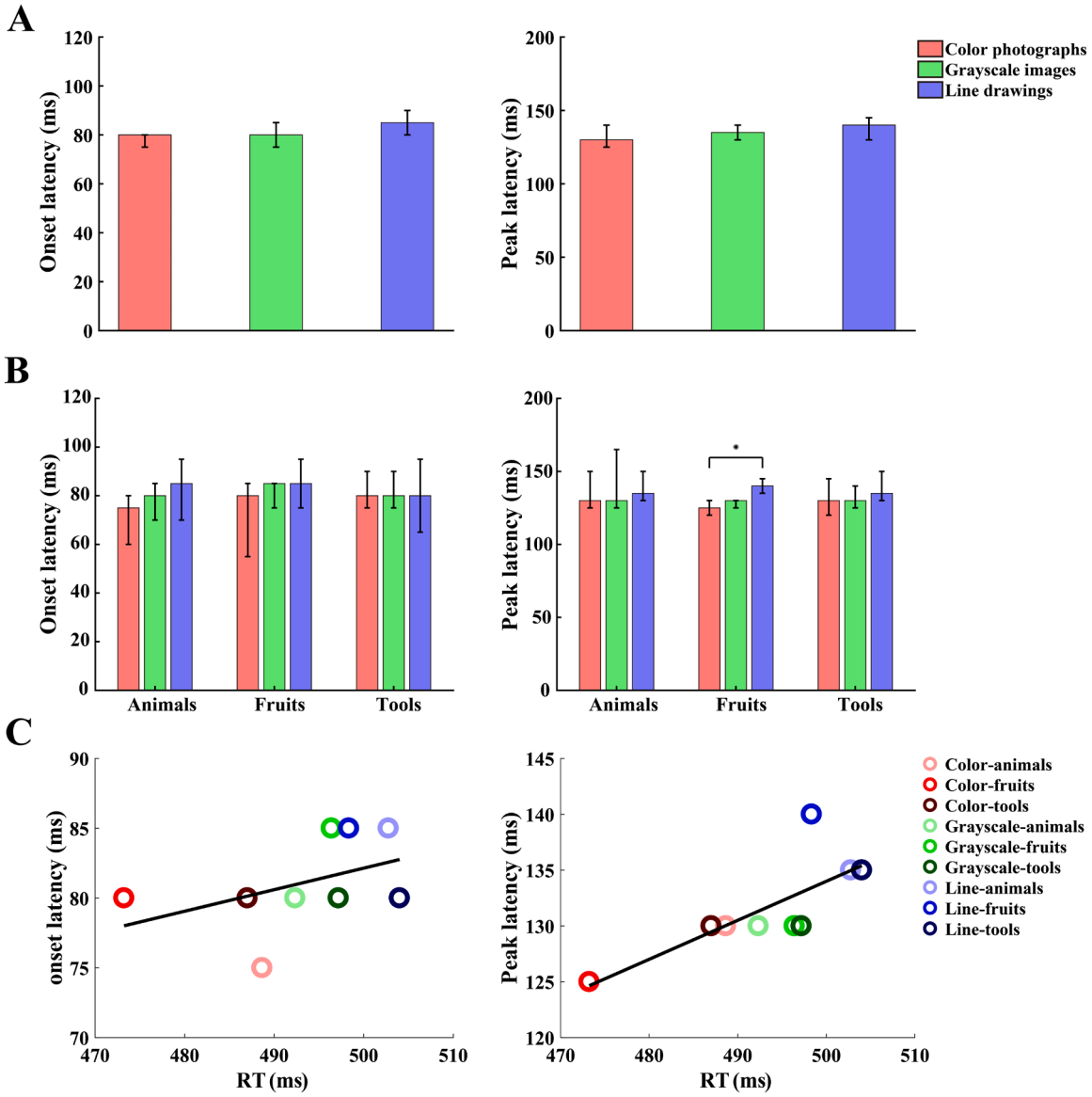

Fig. 5. (A) Onset latency (left) and peak latency (right) of the time-course decoding for three versions of images. (B) Onset latency and peak latency for different objects. Error bars depict bootstrapped 95 % CI. *$p < 0.05$ (two-tailed, FDR corrected). (C) Linear correlation between the RT, onset latency (left), and peak latency (right). The onset latency was not correlated (Pearson's $R = 0.439$, $p = 0.237$), while the peak latency was positively correlated (Pearson's $R = 0.765$, $p = 0.019$).

(Fig. 5B). This revealed a faster peak latency for fruits in color images than for fruits in line drawings ($p = 0.038$; two-tailed bootstrap test, FDR-corrected). No other significant differences were observed. Additionally, we correlated onset latency and peak latency with participants' RTs for the behavioral task, using the bootstrap test to assess significance (Fig. 5C). Although no correlation between the onset latency and RTs was found (Pearson's $R = 0.439$, $p = 0.237$), the peak latency was positively correlated with RTs (Pearson's $R = 0.765$, $p = 0.019$).

To evaluate the role of color information, we also examined neural activities involved in decoding individual object from a grayscale image versus that from a color photograph (Fig. 6A). To this end, we trained a classifier to discriminate neural activities elicited by a color photograph or the grayscale version of the same object. As color was the only difference between the two versions of the same object, if the decoding accuracy is significantly above chance, it would indicate that color information played a role in object recognition. When all object categories were analyzed together, the results revealed that the decoding accuracy was significantly above chance between 110-145 ms for color information (see Fig. 6B). However, separate analysis for each object category revealed that the decoding accuracy was significantly above the chance around 85-440 ms only for fruits, but not for animals and tools, suggesting that color information did not influence neural representations for animals and tools (Fig. 6C).

Using the same method, we also evaluated how other surface information contributed to object representations by decoding neural activities for grayscale images versus those for line drawings at the individual object level. As the two versions of stimuli only differed in the other surface information, an above chance decoding accuracy would suggest a contribution of this information. When all object categories were analyzed together, results showed above-chance decoding accuracy around 75-480 ms for surface information (see Fig. 6B). Similar results were found when the three object categories were analyzed separately. All object types surpassed chance-level decoding accuracy around 80-425 ms (Fig. 6D), indicating a similar role of other surface information across the time course for all three object categories.

3.3. Results of spatial decoding analysis

To investigate which electrodes contributed to the significant decoding of the three versions of pictures, we used the time window of 60 ms to analyze each electrode independently. Fig. 7 shows the decoding accuracy distribution in each sliding time window. As can be seen from this figure, the electrodes throughout the entire brain during the early time window of 81-140 ms contributed to decoding. This persisted until the time window of 441-500 ms. Compared with the time window of 261-320 ms, the decoding accuracy of the electrodes over the posterior occipital lobe was higher in the time window of 321-380 ms, where color photographs created the highest decoding accuracy whereas line drawings created the lowest decoding accuracy.

3.4. Results of time generalization analysis

To examine whether there was a similar neural activity for three versions of images, the time generalization analysis was conducted. Fig. 8 shows the results of this in a time-time matrix of -100-700 ms. The diagonal of the matrices corresponded to the standard time-resolved decoding results. The decodable non-diagonal effect reflected the temporal asynchrony of information processing in the training set and the testing set. When grayscale images were used as the training set and color photographs were used as the testing set (see Fig. 8A), the best decoding accuracy did not shift from the matrix's diagonal, indicating that color did not influence the speed of object neural representations. However, when the grayscale images were the training set and the line drawings were the testing set (see Fig. 8B), there was a shift in the best decoding accuracy relative to the matrix's diagonal. Specifically, the time corresponding to the best decoding accuracy for grayscale images was 10 ms earlier than for line drawings. The results suggest that although color photographs, grayscale images, and line drawings

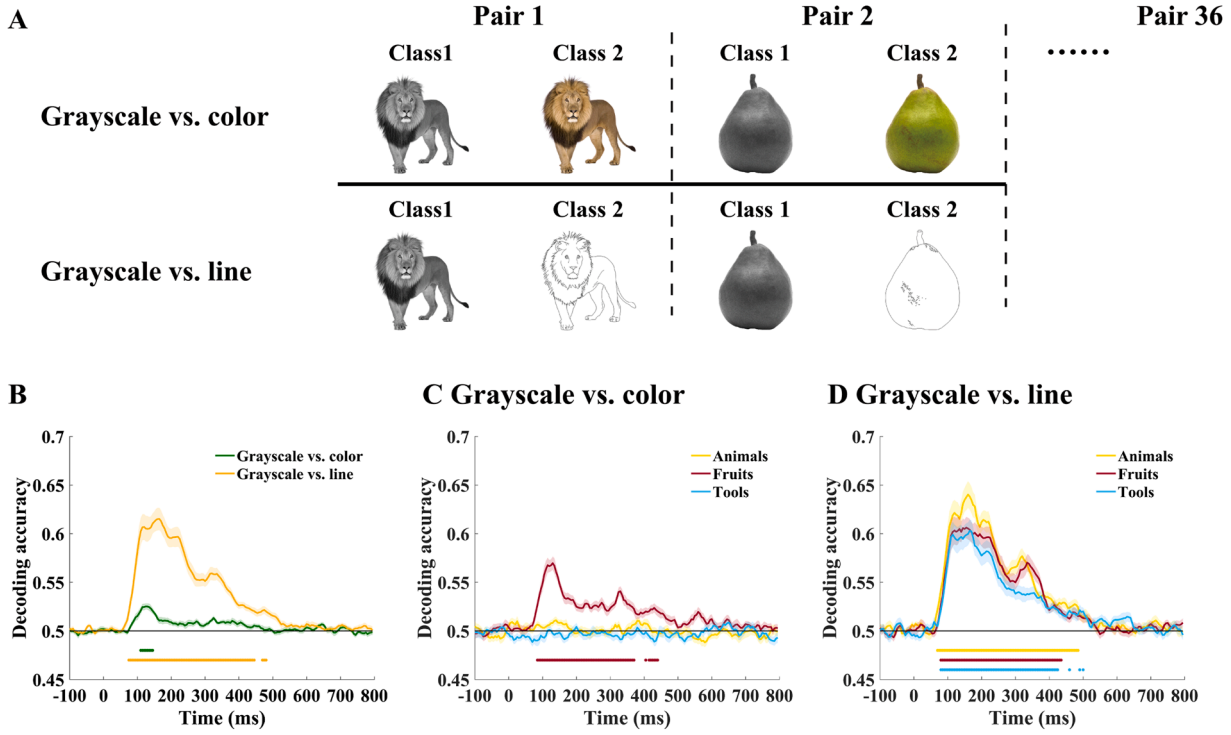

Fig. 6. (A) A classifier was trained to discriminate neural activities elicited by color photographs and grayscale images or by grayscale images and line drawings. Results of decoding accuracy for color photographs vs. grayscale images and grayscale images vs. line drawings for total (B). Results of decoding accuracy for color photographs vs. grayscale images for each category (C) and for grayscale images vs. line drawings for each category (D). Color points below plots indicate time points when decoding accuracy was significantly (TFCE, corrected significance level $p < 0.05$). The shaded areas represent SE about the means.

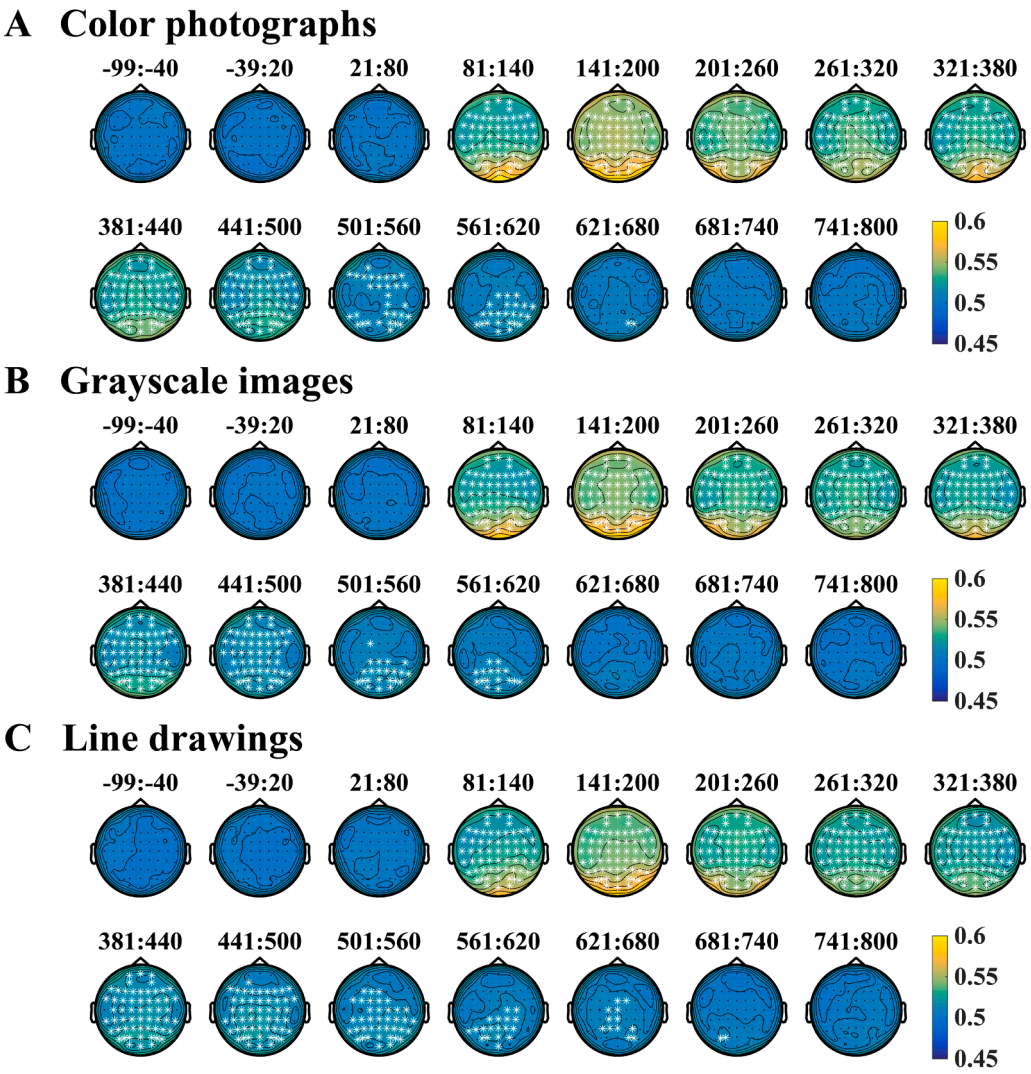

Fig. 7. Decoding accuracy distribution for color photographs (A), grayscale image (B), and line drawings (C). Each distribution map shows the decoding accuracy for each electrode in a given time window. White stars indicated electrodes which decoding accuracy was significantly (TFCE, corrected significance level $p < 0.05$).

elicited similar neural activities, surface information other than color accelerated the object processing speed. Fig. 8C shows the decoding accuracy for the same training set time and testing set time. When color photographs were used as the testing set, significant decoding began at 80 ms, while with line drawings as the testing set, significant decoding began at 95 ms.

4. Discussion

We combined MVPA and EEG methods to investigate the roles of edge-based and surface-based information in the dynamic development of neural representations of visual objects in the brain. The results revealed no significant difference in time-resolved decoding of the neural activities elicited by the three versions of images in the 175-305 ms time window, indicating similar neural representations for all three versions of images during this period. We also found that the surface information from grayscale images modulated neural representations for all three types of objects at the initial stage, but color did not affect the representations of animals and tools. Interestingly, although neural activity decoding could be generalized from grayscale images to either color photographs or line drawings, the best decoding accuracy for the former was on the diagonal, while the latter was offset from diagonal of the matrices, indicating slower neural activity for line drawings than for grayscale images. These results demonstrate how the neural representation of edge-based and surface-based information evolves over time.

Our results provide neural evidence that line drawing elicits similar neural activities to color photographs and grayscale images in a dynamic time course. The time-resolved decoding of three versions of images reached significance from 80-85 ms and reached the first peak at 130-140 ms, which is consistent with the previous MEG/EEG findings on decoding of neural activities of object recognition (Cichy et al., 2014; Contini et al., 2017; Proklova et al., 2019). Peak latency and behavioral response times were positively correlated, indicating that peak latency can predict the speed of one-back performance. Importantly, we found no significant difference in time-resolved decoding of the three versions of images in the 175-305 ms time window, indicating that similar neural representations were elicited by the three types of images during this period.

To further examine whether there were similar neural activities for the three versions of images, we trained a classifier on the neural activities elicited by grayscale images, then generalized the classifier to recognize the three object types in color photographs or line drawings in a time generalization analysis. The results showed that the neural activity pattern could be generalized from grayscale images to both line drawings and color photographs in the entire time process of object representations, providing direct evidence that the three versions had similar the structures in multidimensional space. This finding is

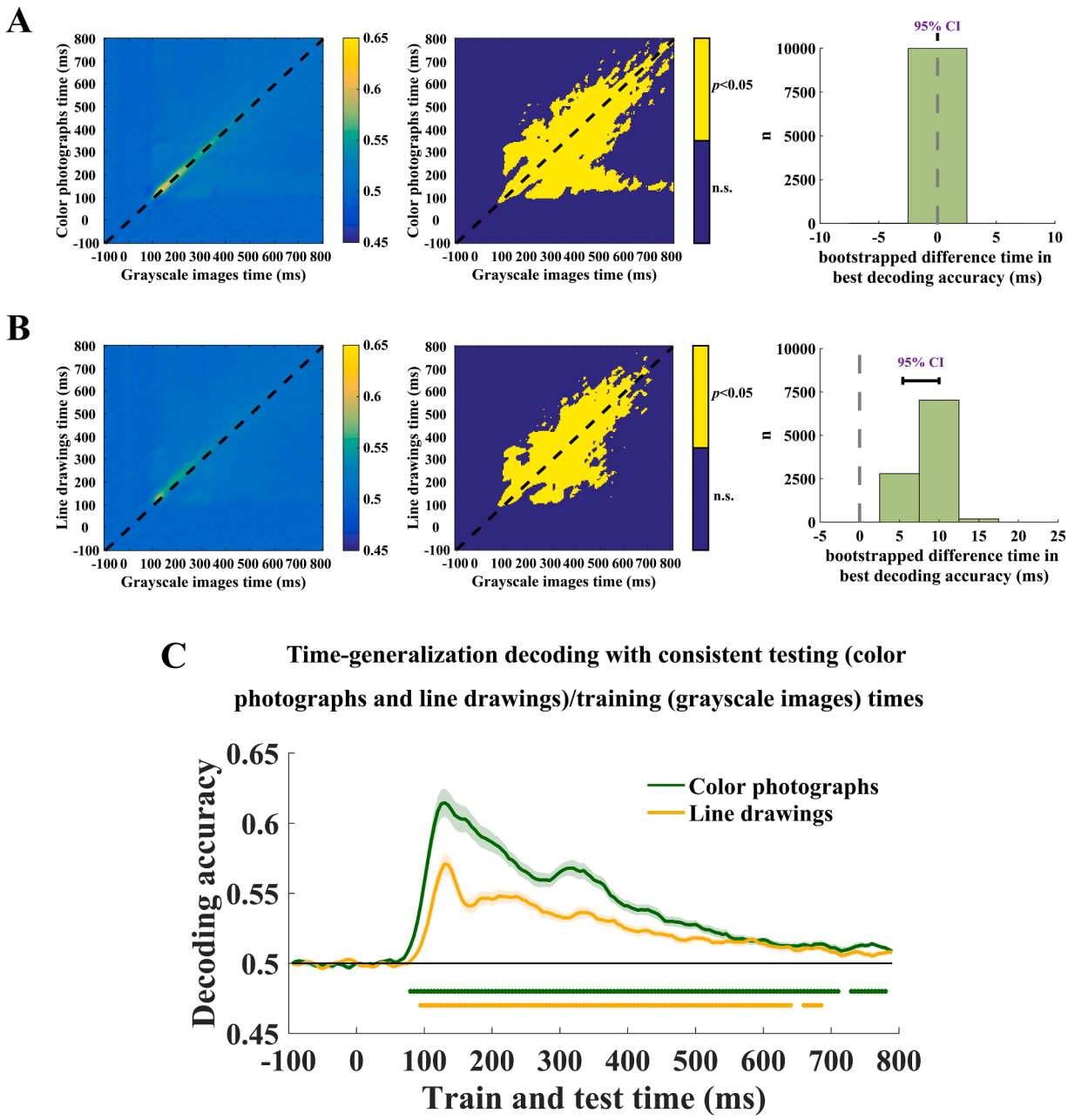

Fig. 8. Results of time generalization analysis for color photographs, grayscale images, and line drawings. (A) Grayscale images were used as the training set, and color photographs were used as the test set. The middle figure shows classification accuracy for each time point combination. The right figure shows the time point combinations (yellow) when decoding accuracy was significant (TFCE, corrected significance level $p < 0.05$), The right shows the bootstrapped differences between the time of training and testing sets corresponding to the best decoding accuracy. (B) Classification accuracy (left), significance (middle) at each time point combination and the bootstrapped difference time (right) in best decoding accuracy when grayscale images were the training set and line drawings were the testing set. (C) Decoding accuracy for the same training set time and testing set time. The line segments below the plots indicate the time points when decoding accuracy were significant (TFCE, corrected significance level $p < 0.05$). Shaded areas represent one SE about the means.

consistent with the prior finding that line drawings and color photographs of six natural scene categories elicit the same activation pattern in the brain areas PPA and RSC (Walther et al., 2011), suggesting that the structural information stored in the line drawings is sufficient to evoke neural representations similar to that of color or grayscale images.

Moreover, our time-resolved decoding results revealed that color might have played a limited role in object representations. We found no significant differences between color photographs and grayscale images in decoding accuracy over different time courses and in neural representations speed in the time generalization analysis results. This finding was consistent with a previous MEG finding showing no difference between the decoding time course of congruently and that incongruently colored objects (Teichmann et al., 2020). Consistently, it was also found that color does not affect object recognition in some previous studies (Bramao et al., 2012; Martinovic et al., 2008; Redmann et al., 2014). However, other research has found that when the shape of the object is ambiguous, color information plays an important role in object recognition (Bramao et al., 2010; Mapelli and Behrmann, 1997; Teichmann et al., 2020). It has also been demonstrated that color is processed in the early stage (P1, N1 components) of object recognition. These results suggest that the role of color in object representations might be modulated by some factors.

To examine how color may influence neural activity for object processing, we decoded neural activities for grayscale images versus color photographs. As color was the only difference between them, if the decoding accuracy is significantly higher than chance, it would indicate that color information played a role in object representations. The results showed that the decoding accuracy for fruits was significantly higher than chance at around 85-440 ms, but this was not the case for animals and tools. This is consistent with the previous finding which also demonstrated the diagnostic value of color for fruits (Rossion and Pourtois, 2004). The reason for this might be that the fruits often have similar shapes (such as roundness) and hence their recognition tends to depend on a diagnostic color. In contrast, animals or tools are more easily distinguished by their shapes. Their colors are often not very useful because many different animals can have very similar colors, such as brown. Hence color information only played a limited role for animals and tools (Price and Humphreys, 1989; Wurm et al., 1993).

We found that surface information other than color plays a role in object representations. When we decoded EEG signals for grayscale images versus for line drawings, the results showed that the decoding accuracy was significantly above the chance level in the time window of 75-480 ms. The onset latency when the other surface information played a role was the same as that of time-resolved decoding of grayscale images, which indicates that the surface information is processed at the initial stage of object recognition. This is consistent with the previous finding that surface information, such as texture modulates P1 composition (Martinovic et al., 2008). Moreover, when comparing the time-resolved decoding results of color photographs, grayscale images, and line drawings, we found that the decoding accuracy for color photographs and grayscale images was significantly higher than that for line drawings at the initial stage (about 90-105 ms) of object representations. These findings suggest the early involvement of surface-based information in object representations.

The time generalization analysis of grayscale images and line drawings also demonstrates that surface information can accelerate the speed of object representations. The results indicate a shift in the best decoding accuracy relative to the diagonal. Specifically, the time corresponding to the best decoding accuracy for line drawing was 10 ms later than for grayscale images. Previous research found that the higher-level visual areas of the temporal lobe were involved in part of the neuronal circuit of object recognition (Albright, 2012; Miyashita, 2004), and the stored conceptual knowledge has an impact about 100 ms after the object presentation (Mudrik et al., 2014; Rahman and Sommer, 2008). The slower processing speed of the line drawings might be due to the lack of surface information in the visual objects, more time was needed to compare the visual stimuli with concept templates in the higher-level brain region and to return feedback signals to the primary visual cortex. Our results provide new electrophysiological evidence that surface-based information influences speed of neural representation of objects.

Interestingly, we found the decoding accuracy of neural activities for line drawings, grayscale images, and color photographs all reached a second peak at 315-335 ms with a posterior scalp distribution. Prior research suggested that the neural activity of 250-400 ms (P3 component) was due to delimit task-extraneous events to focus on attention and promote the memory operation (Polich, 2007). Especially, the neural activity at 315-335 ms with a posterior scalp distribution is called the P3b component, which is caused by attention resources that promote memory operations (Katayama and Polich, 1998; Volpe et al., 2007). Thus, the second peak in our finding could be related to comparing the incoming stimuli with the memory of previously seen stimuli in the working memory. Furthermore, our results indicated that accuracy at the second peak was highest for color photographs, followed by grayscale images, and lowest for line drawings. This might be because color photographs contain more feature elements with greater complexity, which required more attentional resources and elicited a stronger neural response. Previous study have found that the P3b component can be modulated by the stimulus complexity (Hu et al., 2022), which depends on the number and types of constituent elements and the way those elements are organized (Nadal et al., 2010).

5. Conclusion

The present study combined MVPA and EEG methods to investigate how neural representations for edge-based and surface-based information evolve over time. We found that line drawings elicited similar neural representations to those of color photographs and grayscale images between 175-305 ms. Furthermore, all three versions of the images had similar multidimensional spatial structures in the brain throughout the object representations process. We also discovered that other surface information rather than color information facilitated decoding accuracy at the initial stage and affected the speed of neural representation of objects. These results provide new insights into the role of edge-based and surface-based information on the dynamic process of neural representations of visual objects.

Data and code availability statement

The available data and code can be found at https://doi.org/10.57760/sciencedb.psych.00185.

CRediT authorship contribution statement

Liansheng Yao: Conceptualization, Data curation, Formal analysis, Investigation, Methodology, Visualization, Writing – original draft, Writing – review & editing. **Qiufang Fu:** Conceptualization, Funding acquisition, Methodology, Project administration, Writing – review & editing. **Chang Hong Liu:** Writing – review & editing.

Declaration of Competing Interest

We declare that we have no financial and personal relationship with other people or organization that can inappropriately influence our work, and there is no professional or other personal interest of any nature or kind in any service or company that could be construed as influencing the review of the manuscript entitled.

Data availability

Data will be made available on request.

Acknowledgements

The research was supported by the National Key Research and Development Program of China (No. 2018AAA0100205), the National Natural Science Foundation of China, the German Research Foundation (NSFC 62061136001/DFG TRR-169).

References

Albright, T.D., 2012. On the perception of probable things: neural substrates of associative memory, imagery, and perception. Neuron 74 (2), 227–245. https://doi.org/10.1016/j.neuron.2012.04.001.

Biederman, I., Ju, G., 1988. Surface versus edge-based determinants of visual recognition. Cognit. Psychol. 20 (1), 38–64. https://doi.org/10.1016/0010-0285(88)90024-2.

Boshyan, J., Barrett, L.F., Betz, N., Adams, R.B., Kveraga, K., 2018. Line-drawn scenes provide sufficient information for discrimination of threat and mere negativity. I-Perception 9 (1), 26. https://doi.org/10.1177/2041669518755806.

Brainard, D.H., 1997. The psychophysics toolbox. Spat. Vis. 10 (4), 433–436. https://doi.org/10.1163/156856897x00357.

Bramao, I., Faisca, L., Petersson, K.M., Reis, A., 2010. The influence of surface color information and color knowledge information in object recognition. Am. J. Psychol. 123 (4), 437–446. https://doi.org/10.5406/amerjpsyc.123.4.0437.

Bramao, I., Francisco, A., Inacio, F., Faisca, L., Reis, A., Petersson, K.M., 2012. Electrophysiological evidence for colour effects on the naming of colour diagnostic and noncolour diagnostic objects. Vis. Cogn. 20 (10), 1164–1185. https://doi.org/10.1080/13506285.2012.739215.

Carlson, T., Tovar, D.A., Alink, A., Kriegeskorte, N., 2013. Representational dynamics of object vision: the first 1000 ms. J. Vis. 13 (10), 19. https://doi.org/10.1167/13.10.1.

Cave, C.B., Bost, P.R., Cobb, R.E., 1996. Effects of color and pattern on implicit and explicit picture memory. J. Exp. Psychol. Learn. Mem. Cogn. 22 (3), 639–653. https://doi.org/10.1037/0278-7393.22.3.639.

Chang, C.C., Lin, C.J., 2011. LIBSVM: a library for support vector machines. ACM Trans. Intell. Syst. Technol. 2 (3) https://doi.org/10.1145/1961189.1961199.

Cichy, R.M., Pantazis, D., Oliva, A., 2014. Resolving human object recognition in space and time. Nat. Neurosci. 17 (3), 455–462. https://doi.org/10.1038/nn.3635.

Contini, E.W., Wardle, S.G., Carlson, T.A., 2017. Decoding the time-course of object recognition in the human brain: From visual features to categorical decisions. Neuropsychologia 105, 165–176. https://doi.org/10.1016/j.neuropsychologia.2017.02.013.

Cree, G.S., McRae, K., 2003. Analyzing the factors underlying the structure and computation of the meaning of chipmunk, cherry, chisel, cheese, and cello (and many other such concrete nouns). J. Exp. Psychol. Gen. 132 (2), 163–201. https://doi.org/10.1037/0096-3445.132.2.163.

de-Wit, L., Alexander, D., Ekroll, V., Wagemans, J., 2016. Is neuroimaging measuring information in the brain? Psychon. Bull. Rev. 23 (5), 1415–1428. https://doi.org/10.3758/s13423-016-1002-0.

Delorme, A., Makeig, S., 2004. EEGLAB: an open source toolbox for analysis of single-trial EEG dynamics including independent component analysis. J. Neurosci. Methods 134 (1), 9–21. https://doi.org/10.1016/j.jneumeth.2003.10.009.

Dobs, K., Isik, L., Pantazis, D., Kanwisher, N., 2019. How face perception unfolds over time. Nat. Commun. 10 https://doi.org/10.1038/s41467-019-09239-1. Article 1258.

Fu, Q.F., Liu, Y.J., Dienes, Z., Wu, J.H., Chen, W.F., Fu, X.L., 2016. The role of edge-based and surface-based information in natural scene categorization: Evidence from behavior and event-related potentials. Conscious. Cogn. 43, 152–166. https://doi.org/10.1016/j.concog.2016.06.008.

Gegenfurtner, K.R., Rieger, J., 2000. Sensory and cognitive contributions of color to the recognition of natural scenes. Curr. Biol. 10 (13), 805–808. https://doi.org/10.1016/s0960-9822(00)00563-7.

Goffaux, V., Jacques, C., Mouraux, A., Oliva, A., Schyns, P.G., Rossion, B., 2005. Diagnostic colours contribute to the early stages of scene categorization: Behavioural and neurophysiological evidence. Vis. Cogn. 12 (6), 878–892. https://doi.org/10.1080/13506280444000562.

Grootswagers, T., Wardle, S.G., Carlson, T.A., 2017. Decoding dynamic brain patterns from evoked responses: a tutorial on multivariate pattern analysis applied to time series neuroimaging data. J. Cogn. Neurosci. 29 (4), 677–697. https://doi.org/10.1162/jocn_a_01068.

Hatamimajoumerd, E., Murty, N.A.R., Pitts, M., Cohen, M.A., 2022. Decoding perceptual awareness across the brain with a no-report fMRI masking paradigm. Curr. Biol. 32 (19) https://doi.org/10.1016/j.cub.2022.07.068, 4139-+.

Hu, R., Zhang, L., Meng, P., Meng, X., Weng, M., 2022. The neural responses of visual complexity in the oddball paradigm: an ERP study. Brain Sci. 12 (4), 447. https://doi.org/10.3390/brainsci12040447.

Katayama, J.i., Polich, J., 1998. Stimulus context determines P3a and P3b. Psychophysiology 35 (1), 23–33. https://doi.org/10.1111/1469-8986.3510023.

Kleiner, M., 2010. Visual stimulus timing precision in psychtoolbox-3: tests, pitfalls and solutions. Perception 39. https://doi.org/10.1177/03010066100390S101, 189-189.

Laws, K.R., 2001. What is structural similarity and is it greater in living things? Behav. Brain Sci. 24 (3), 486–487. https://doi.org/10.1017/S0140525X01324159.

Laws, K.R., Hunter, M.Z., 2006. The impact of colour, spatial resolution, and presentation speed on category naming. Brain Cogn. 62 (2), 89–97. https://doi.org/10.1016/j.bandc.2006.03.002.

Lloyd-Jones, T.J., Roberts, M.V., Leek, E.C., Fouquet, N.C., Truchanowicz, E.G., 2012. The time course of activation of object shape and shape plus colour representations during memory retrieval. PLoS One 7 (11), 12. https://doi.org/10.1371/journal.pone.0048550.

Lowe, M.X., Rajsic, J., Gallivan, J.P., Ferber, S., Cant, J.S., 2017. Neural representation of geometry and surface properties in object and scene perception. Neuroimage 157, 586–597. https://doi.org/10.1016/j.neuroimage.2017.06.043.

Macmillan, N.A., Creelman, C.D., 1991. Detection Theory: A User's Guide. Cambridge University Press.

Mapelli, D., Behrmann, M., 1997. The role of color in object recognition: evidence from visual agnosia. Neurocase 3 (4), 237–247. https://doi.org/10.1080/13554799708405007.

Martinovic, J., Gruber, T., Muller, M.M., 2008. Coding of visual object features and feature conjunctions in the human brain. PLoS One 3 (11), 10. https://doi.org/10.1371/journal.pone.0003781.

Miyashita, Y., 2004. Cognitive memory: cellular and network machineries and their top-down control. Science 306 (5695), 435–440. https://doi.org/10.1126/science.1101864.

Mudrik, L., Shalgi, S., Lamy, D., Deouell, L.Y., 2014. Synchronous contextual irregularities affect early scene processing: replication and extension. Neuropsychologia 56, 447–458. https://doi.org/10.1016/j.neuropsychologia.2014.02.020.

Nadal, M., Munar, E., Marty, G., Cela-Conde, C.J., 2010. Visual complexity and beauty appreciation: explaining the divergence of results. Empir. Stud. Arts 28 (2), 173–191. https://doi.org/10.2190/EM.28.2.d.

Nemrodov, D., Niemeier, M., Mok, J.N.Y., Nestor, A., 2016. The time course of individual face recognition: a pattern analysis of ERP signals. Neuroimage 132, 469–476. https://doi.org/10.1016/j.neuroimage.2016.03.006.

Oosterhof, N.N., Connolly, A.C., Haxby, J.V., 2016. CoSMoMVPA: multi-modal multivariate pattern analysis of neuroimaging data in Matlab/GNU Octave. Front. Neuroinform. 10, 27. https://doi.org/10.3389/fninf.2016.00027.

Parron, C., Washburn, D., 2010. Contrasting the edge- and surface-based theories of object recognition: behavioral evidence from macaques (Macaca mulatta). J. Exp. Psychol. Anim. Behav. Process. 36 (1), 148–157. https://doi.org/10.1037/a0015629.

Polich, J., 2007. Updating P300: an integrative theory of P3a and P3b. Clin. Neurophysiol. 118 (10), 2128–2148. https://doi.org/10.1016/j.clinph.2007.04.019.

Price, C.J., Humphreys, G.W., 1989. The effects of surface detail on object categorization and naming. Q. J. Exp. Psychol. 41 (4), 797–828. https://doi.org/10.1080/14640748908402394.

Proklova, D., Kaiser, D., Peelen, M.V., 2019. MEG sensor patterns reflect perceptual but not categorical similarity of animate and inanimate objects. Neuroimage 193, 167–177. https://doi.org/10.1016/j.neuroimage.2019.03.028.

Rahman, R.A., Sommer, W., 2008. Seeing what we know and understand: how knowledge shapes perception. Psychon. Bull. Rev. 15 (6), 1055–1063. https://doi.org/10.3758/pbr.15.6.1055.

Redmann, A., FitzPatrick, I., Hellwig, F., Indefrey, P., 2014. The use of conceptual components in language production: an ERP study. Front. Psychol. 5 https://doi.org/10.3389/fpsyg.2014.00363.

Robin, J., Lowe, M.X., Pishdadian, S., Rivest, J., Cant, J.S., Moscovitch, M., 2017. Selective scene perception deficits in a case of topographical disorientation. Cortex 92, 70–80. https://doi.org/10.1016/j.cortex.2017.03.014.

Rossion, B., Pourtois, G., 2004. Revisiting Snodgrass and Vanderwart's object pictorial set: the role of surface detail in basic-level object recognition. Perception 33 (2), 217–236. https://doi.org/10.1068/p5117.

Rousselet, G., Pernet, C., 2011. Quantifying the time course of visual object processing using ERPs: it's time to up the game [perspective]. Front. Psychol. 2 https://doi.org/10.3389/fpsyg.2011.00107.

Sanchez, G., Hartmann, T., Fusca, M., Demarchi, G., Weisz, N., 2020. Decoding across sensory modalities reveals common supramodal signatures of conscious perception. Proc. Nat. Acad. Sci. U. S. A. 117 (13), 7437–7446. https://doi.org/10.1073/pnas.1912584117.

Scholl, C.A., Jiang, X., Martin, J.G., Riesenhuber, M., 2014. Time course of shape and category selectivity revealed by EEG rapid adaptation. J. Cogn. Neurosci. 26 (2), 408–421. https://doi.org/10.1162/jocn_a_00477.

Schyns, P.G., Oliva, A., 1994. From blobs to boundary edges: evidence for time-and spatial-scale-dependent scene recognition. Psychol. Sci. 5 (4), 195–200. https://doi.org/10.1111/j.1467-9280.1994.tb00500.x.

Smith, F.W., Smith, M.L., 2019. Decoding the dynamic representation of facial expressions of emotion in explicit and incidental tasks [Article]. Neuroimage 195, 261–271. https://doi.org/10.1016/j.neuroimage.2019.03.065.

Smith, S.M., Nichols, T.E., 2009. Threshold-free cluster enhancement: addressing problems of smoothing, threshold dependence and localisation in cluster inference. Neuroimage 44 (1), 83–98. https://doi.org/10.1016/j.neuroimage.2008.03.061.

Stelzer, J., Chen, Y., Turner, R., 2013. Statistical inference and multiple testing correction in classification-based multi-voxel pattern analysis (MVPA): random permutations and cluster size control. Neuroimage 65, 69–82. https://doi.org/10.1016/j.neuroimage.2012.09.063.

Teichmann, L., Quek, G.L., Robinson, A.K., Grootswagers, T., Carlson, T.A., Rich, A.N., 2020. The influence of object-color knowledge on emerging object representations in the brain. J. Neurosci. 40 (35), 6779–6789. https://doi.org/10.1523/jneurosci.0158-20.2020.

Volpe, U., Mucci, A., Bucci, P., Merlotti, E., Galderisi, S., Maj, M., 2007. The cortical generators of P3a and P3b: a LORETA study. Brain Res. Bull. 73 (4-6), 220–230. https://doi.org/10.1016/j.brainresbull.2007.03.003.

Walther, D.B., Chai, B., Caddigan, E., Beck, D.M., Fei-Fei, L., 2011. Simple line drawings suffice for functional MRI decoding of natural scene categories. Proc. Nat. Acad. Sci. U. S. A. 108 (23), 9661–9666. https://doi.org/10.1073/pnas.1015666108.

Wurm, L.H., Legge, G.E., Isenberg, L.M., Luebker, A., 1993. Color improves object recognition in normal and low vision. J. Exp. Psychol. Hum. Percept. Perform. 19 (4), 899–911. https://doi.org/10.1037/0096-1523.19.4.899.

Zachariou, V., Del Giacco, A.C., Ungerleider, L.G., Yue, X.M., 2018. Bottom-up processing of curvilinear visual features is sufficient for animate/inanimate object categorization. J. Vis. 18 (12), 12. https://doi.org/10.1167/18.12.3.